Sustainable Energy, Grids and Networks 43 (2025) 101754

Contents lists available at ScienceDirect

Sustainable Energy, Grids and Networks

journal homepage: www.elsevier.com/locate/segan

The energy aggregator problem – A holistic mixed-integer linear programming approach ☆

Kai Hoth [a,*], Béla Wiegel [b], Tizian Schug [a], Kathrin Fischer [a]

[a] Institute for Operations Research and Information Systems of Hamburg University of Technology, 21073 Hamburg, Germany
[b] Institute for Electrical Power and Energy Technology of Hamburg University of Technology, 21079 Hamburg, Germany

ARTICLE INFO

Keywords:
Aggregator
Energy storage
Heat pump
Local energy market
Renewable energy
Smart grid
Transactive energy

ABSTRACT

In this paper, a new mixed integer linear programming (MILP) model for the day-ahead operation of energy aggregators (EA) is developed. Synergies between the different types of flexibility and energy trading options enable EAs in decentralized and renewable energy systems to provide economic benefits to participating households but require a detailed consideration of technological properties and constraints of the respective types of resources. Therefore, the main contribution of this work is the development of a new EA model (EAM), which combines a holistic perspective with a high level of technical detail to better address the complexity of the EA decision. Most importantly, power-to-heat systems are integrated with their inherent thermal relations between heat pumps, heater rods and heat storages. In combination with other energy resources such as photovoltaic systems, electric vehicles, household battery storages and time-shiftable loads, households are modeled as systems with interdependent electrical power and heat flows. Moreover, three different trading levels (wholesale, local markets and internal trading) are taken into account. The model application to a case study with up to 111 individually modeled prosumer households in a summer and a winter scenario reveals high synergetic potential of EAs resulting from the flexibility of multiple trading options in combination with the flexibility of various energy resources. The results validate the efficacy of the model, as significant economic benefits for households are realized in comparison to a base case of non-aggregated households, showing that the three trading levels significantly contribute to these benefits. Further analyses give insights into the interdependent synergetic relations between different flexible resources, underlining the importance of a holistic optimization approach that explicitly takes these relations into account. For future research, the EAM is proposed as a base model to depict the behavior of EAs.

1. Introduction

The concept of Energy Aggregators (EAs) is a widely discussed research topic as an approach for coping with the opportunities and challenges of future energy systems [1–3]. Efficiently coordinating the intermittency of renewable energy sources (RESs) with the flexibility provided by different types of distributed energy resources (DERs) among large numbers of prosumer households, constitutes a complex and multi-faceted decision problem. A newly developed holistic mixed-integer linear programming (MILP) approach to this EA problem is presented in this work which, in addition to multiple types of flexible DERs and trading options, integrates power-to-heat (P2H) systems at a high level of detail.

The proposed day-ahead Energy Aggregator Model (EAM) considers an EA that performs energy management for a large number of local prosumer households, by scheduling their respective DERs such as electric vehicles (EVs), household battery storage systems (BSs), P2H systems or time-shiftable loads (TSLs) under consideration of residential photovoltaic (PV) energy generation and inflexible loads. Energy trading is conducted on behalf of the households and in correspondence with the scheduling decisions with the objective of maximizing the total trading profit for all households. Apart from two external trading options on wholesale market (WS) level and a local market (LM), the aggregated

☆ Paper submitted on 05.11.2024. The authors gratefully acknowledge financial support by the Ministry for Science, Research, Equality and Districts Authority, Hamburg, Germany.

* Corresponding author.
Email addresses: kai.hoth@tuhh.de (K. Hoth), bela.wiegel@tuhh.de (B. Wiegel), tizian.schug@tuhh.de (T. Schug), kathrin.fischer@tuhh.de (K. Fischer).

https://doi.org/10.1016/j.segan.2025.101754
Received 5 November 2024; Received in revised form 14 February 2025; Accepted 18 May 2025
Available online 20 May 2025

households are interconnected through internal trading, thereby forming an energy community (EC). To account for the distinct technological properties, a high level of detail regarding the constraints for the operation of different types of DERs is considered in the model. An important contribution lies in the detailed modeling of P2H systems, consisting of a heat pump (HP), a heater rod (HR) and a heat storage (HS) with the respective thermal relations, whilst also modeling the household itself as a thermal system. This model is applied in a case study for a summer and a winter scenario with 62 days, respectively. The results show the economic benefit that EAs are able to provide to prosumer households as a consequence of holistically and interdependently exploiting multiple trading options and flexibly scheduling DERs. The respective potential of the different trading options and the different types of DERs is further analyzed, revealing interdependent effects between their specific characteristics and, thus, supporting the holistic modeling approach to the EA problem.

The remainder of the paper is organized as follows. In Section 2, the basics of the EA concept and the resulting decision problem are introduced in the course of a literature review regarding previous related works on EAs. Section 3 presents the model in detail, followed by an overview of the case study in Section 4. In Section 5, the results of the case study are presented, analyzed and discussed. The paper ends with a conclusion and an outlook on future research in Section 6.

2. Energy aggregators

This section first provides an overview of the general concept of EA, before presenting a literature review with a more detailed consideration of related modeling approaches on which this work builds up.

2.1. Concept of energy aggregators

The trend towards renewable, decentralized and digitized energy systems presents challenges as well as opportunities with regard to architecture and operation [1,2]. On the one hand, building on the potential of a sophisticated information and communication technology infrastructure, smart grids enable new operational concepts for energy systems by facilitating frequent communication and providing a high availability of information [4]. On the other hand, the volatility of RESs and the increasing complexity due to a high number of DERs require efficient and resilient energy management strategies [5,6]. An adequate design of energy markets must allow the participation of residential prosumers and consumers to fully utilize their DERs in accordance with these opportunities and challenges [1,7]. Transactive control describes a framework to exert influence of grid operators on energy trading by means of price signals that consider the system objectives of resilience and sustainability [8–10]. Especially in LMs, energy trading can accordingly be done under consideration of local grid states [11]. Thus, line congestions or voltage violations can be mitigated through market processes [12,13]. LMs represent an additional trading platform next to WS trading with comparatively limited trading options due to their smaller size [14]. In addition to energy markets, ancillary services such as local flexibility procurement for system operators enable further possibilities to exploit DERs with regard to system objectives [15].

Operating a smart grid with the above characteristics requires a sophisticated energy management of the respective DERs. EAs can efficiently perform this task on behalf of a large EC of residential prosumers in a way that is beneficial to all participants [1,16,17]. Not only in research, but also in practice the notion of EC is becoming increasingly relevant, as the Energy Communities Repository and the Rural Energy Communities Advisory Hub by the European Commission show [18,19]. An overview of the roles and functions of EAs is given in Fig. 1 which shows that EAs are the interface between residential prosumers and energy markets [20,21]. Accordingly, they can deploy DERs in a way that takes advantage of energy price fluctuations, and also create synergies by aggregating the flexibility of different DERs, thus widening the range of interactive scheduling and trading options [22]. The synergies build

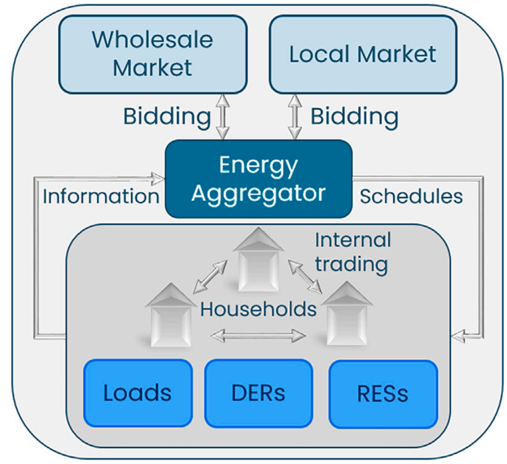

Fig. 1. EA concept.

on internal trading between prosumers within an EC which is centrally managed by the respective EA [23]. On household level, individual prosumers profit by consuming energy cost-efficiently and monetizing their self-generated power and the flexibility of their DERs [16].

2.2. The energy aggregator problem – literature overview

The role of EAs comprises a variety of interdependent decision problems, mainly the scheduling of different types of DERs and the trading and balancing of energy [24]. Due to the broadness and complexity of the general problem, previous optimization approaches have focused on specific aspects, thus neglecting other major aspects, e.g. specific types of DERs such as HPs [1,14,24–30]. The scheduling of DERs is an aspect that is multi-faceted in itself, as there are different types of DERs with specific technical and practical restrictions. Previous works feature aggregators that integrate the basic types of DERs such as PV or solar thermal (ST) systems, EVs, BSs and TSLs on a limited level of technical detail [13,14,29,31–33]. With only slight variations, these works similarly consider basic aspects such as power and capacity restrictions and SOC-balancing for storages, driving demands of EVs or the temporal shifting of uninterruptible power profiles within fixed time windows for TSLs.

Due to the high complexity and partial non-linearity of the thermodynamic relations, optimizing the operation of a P2H system with an HP, HS and HR under consideration of temperature preferences and warm water demands (WW) in a detailed and efficient way presents a challenging task. Accordingly, an overview of previous EA-related works reveals that the consideration of heat systems is sparsely represented [1]. Few previous comprehensive optimization approaches integrate P2H systems in a simplified way by assuming a constant coefficient of performance (COP) or energy efficiency ratio (EER) and by neglecting heat storages and thus, the inherent thermodynamic relations, as well as other heat transmissions and losses [31,34,35]. Since P2H systems have the potential to provide significant contributions by realizing synergies between the flexibility of different types of DERs, modeling them in a comprehensive and sophisticated manner constitutes an important research problem [36–38]. This research gap is addressed in this work by introducing a model which integrates P2H systems together with a variety of different DER types at a high level of technical detail.

Apart from the scheduling of different types of DERs, energy trading represents another major function of EAs [13]. Trading can generally be done on external or internal level. In order to deploy market mechanisms that exploit the DERs while considering local grid states, EAs may externally participate in LMs in addition to WS energy trading

[14,37,39–42]. Integrating both external trading options with their respective exogenous energy prices and trading fees, and also considering household-specific energy allocation in the form of internal trading, further increases the complexity of the EA problem [16]. A common and valid assumption in previous works is that EAs act as price takers that submit purchasing or selling bids without exerting influence on the exogenous prices [1,24]. This restricts the bidding decisions to specifying the time and the offered or requested energy amounts.

3. The energy aggregator model

In the following section, the EAM is presented. For a better overview, the different constraint groups are split into separate categories that represent the different components of the EA problem. Whereas the technical constraints for the operation of P2H systems are newly developed in this work, the respective constraints regarding EVs, BSs and TSLs are in line with previous optimization approaches (see Section 2.2) and adapted accordingly to the EAM.

3.1. Model assumptions

A schematic overview of the different system components of the EA problem at the household (HH) level is presented in Fig. 2 and illustrates the interrelations between the various decision problems in the way they are addressed in this work. Two external trading options are considered at the WS and LM levels. A basic assumption is that EAs act as price takers at the external level. At the internal level, the assumption is made that respective energy price equals the higher of the two external prices at a given time. Consequently, selling energy internally is equivalent to realizing the more profitable external selling option, thus ensuring that trading internally does not require selling households to miss out on more profitable external trading options (i.e. to make sure that rational households will actually engage in internal trading). A formal description for ensuring that internal trade can only take place if it is also beneficial for the purchasing household follows in (2) below. Furthermore, trading fees, including grid access charges and taxes, are only considered for energy purchases as an approach to assign fees to consumers [43]. It is assumed that WS fees are higher than LM fees, which, in turn, are higher than internal trading fees, to represent a subsidy for lower-level trading in order to reduce inter-regional power flow and hence ensure grid stability. The system perspective of EAs requires all scheduling and trading decisions to be made interdependently, as the power and heat flows of each household have to be balanced at all times (see Fig. 2).

Thus, the EA problem consists of efficiently scheduling all DERs in accordance with their respective technological constraints, and submitting market bids in compliance with the household power and heat balances. The inherent flexibility is used to efficiently trade energy, but the option

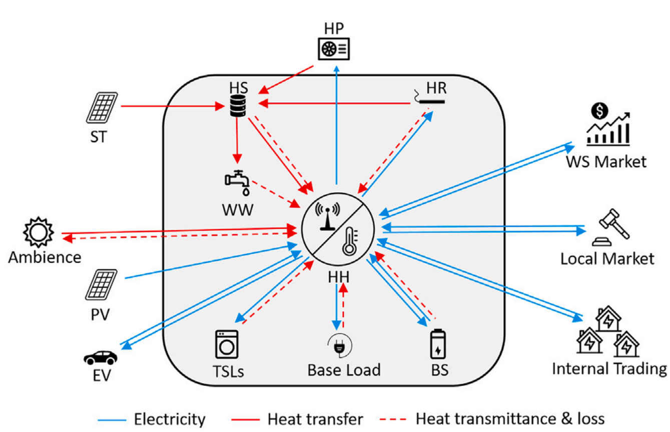

Fig. 2. EA Problem on household level.

of providing external flexibility services is not considered. Furthermore, the model builds on the assumption that households already possess DERs and are willing to enable an exterior system actor to manage the operation of these resources. This follows the assumption that, by realizing synergies due to aggregation, such an entity is able to perform more efficient energy management than households would be able to do without an EA. An EA is not only able to efficiently schedule DERs, but also enables households to participate in the different energy markets and exploit the inherent price differences.

To enable a better understanding of the following model description, an overview of all sets, variables and parameters is provided in Tables 2, 3 and 4 in the Appendix. In these tables, the frequently occurring indices h and t represent specific households and time steps. For reasons of clarity, explanations of these indices are excluded from the respective definitions.

3.2. Objective: total trading profit maximization

The behavior of EAs is driven by the economic objective of trading profit maximization for all households in the EC [1]. In line with previous works, this is represented in the objective function in (3), which maximizes the total trading profit of the EC [31,34]. The variables P constitute the electric power traded on behalf of prosumer households H on each of the three trading levels (WS, LMs and internal) at time step t in the planning horizon T. The parameters λ and f denote the market prices and fees, respectively. For internal trading, only the fees on the purchaser side are considered as the prices on purchaser and seller side cancel each other out. As prices and fees relate to energy and not to power, the term is multiplied with the time step width Δt. Due to sign convention in power flow, purchasing is represented by positive signs and selling by negative signs. Consequently, a positive objective function value indicates a loss and a negative one a profit, thus formally resulting in a minimization function. The binary parameters Λ contain the information if trading on LMs or internal level is enabled. Accordingly, Λ^{LM} is only assigned a value of 1 if the structure of prices and fees is such that local trading is beneficial for the purchasing and selling side in comparison to WS trading. This is formally declared in (1).

$$\Lambda_t^{LM} = \begin{cases} 1, & \text{if } \lambda_t^{WS} \leq \lambda_t^{LM} \leq \lambda_t^{WS} + f^{WS} - f^{LM} \\ 0, & \text{else} \end{cases} \tag{1}$$

The binary parameter Λ^{int} is determined in accordance with (2) to ensure that internal trading can only take place if it is beneficial for the purchasing and the selling household.

$$\Lambda_t^{int} = \begin{cases} 1, & \text{if} \max\left(\lambda_t^{WS}, \quad \lambda_t^{LM}\right) + f^{int} \leq \\ & \quad \min\left(\lambda_t^{WS} + f^{WS}, \quad \lambda_t^{LM} + f^{LM}\right) \\ 0, & \text{else} \end{cases} \tag{2}$$

Only in the cases when the Λ parameters have a value of 1, the respective trading options are considered by the EA and hence become part of the optimization, i.e. it is decided by the model how much energy is traded on the respective market.

$$\begin{aligned} \min \sum_{t \in T} \sum_{h \in H} \Big[& P_{h,t}^{WS,buy} \cdot \left(\lambda_t^{WS} + f^{WS}\right) - P_{h,t}^{WS,sell} \cdot \lambda_t^{WS} \\ & + \left(P_{h,t}^{LM,buy} \cdot \left(\lambda_t^{LM} + f^{LM}\right) - P_{h,t}^{LM,sell} \cdot \lambda_t^{LM}\right) \cdot \Lambda_t^{LM} \\ & + P_{h,t}^{int,buy} \cdot f^{int} \cdot \Lambda_t^{int} \Big] \cdot \Delta t \end{aligned} \tag{3}$$

3.3. Power-to-heat systems

Modeling the operation of P2H systems constitutes a high level of complexity. The following sets of newly developed constraints, integrated into the general day-ahead energy management of an EA, present the EAM's main contribution. As a simplification, the operation is modeled for two different cases in which an air–water–HP is in either heating or cooling mode for the whole planning period T. Both operative modes result in a distinct variant of the EAM. The respective constraints for both cases are presented in this section. In order to reduce computational complexity and simultaneously avoiding the problem of short-term erratic behavior in the operation of HPs, all operative decisions are considered for $t \in T^{HP} \subseteq T$ with the time step width Δt^{HP} and the ratio of different time step widths $\Pi^{HP} = \frac{\Delta t^{HP}}{\Delta t}$. H' represents the set of households with a P2H system.

3.3.1. Heating mode

The resulting heat flow $\dot{Q}$ from a HP is linearly related to the operating power P^{HP} for a constant COP. However, the COP itself is non-linearly dependent on P^{HP} and the difference between the HP's supply temperature and the ambient temperature ϑ^{amb}. In order to model this relation linearly, the heat flow is predetermined for defined levels of the operating power and intervals of the temperature difference. This results in the parameter matrix $\dot{Q}^{fix}$ for all possible operational modes Ω. The variable $\dot{Q}$ is assigned a value from this matrix in (4) with the help of a binary variable γ^{HP} which is limited to a single operational mode of operating power level i and temperature difference interval j in (5). However, the supply temperature is not modeled explicitly. As a simplification, the calculations of $\dot{Q}^{fix}$ assume a constant temperature offset of 5 K between the supply temperature and the modeled HS temperature ϑ^{HS}. The binary parameter Γ^{HP} ensures that a HP is only deployable if the ambient temperature is within the operational limits under consideration of the bivalence point. This is determined a priori.

$$\dot{Q}^{HP}_{h,t} = \sum_{i,j\in\Omega_h} \left(\gamma^{HP}_{h,t,i,j} \cdot \dot{Q}^{fix}_{h,i,j}\right) \cdot \Gamma^{HP}_{h,t} \quad \forall \quad h \in H', t \in T^{HP} \tag{4}$$

$$\sum_{i,j\in\Omega_h} \gamma^{HP}_{h,t,i,j} \le 1 \quad \forall \quad h \in H', t \in T^{HP} \tag{5}$$

Accordingly, the operating power is set to the respective level of P^{fix} in (6) and the HS temperature is limited to the respective interval with the upper bound $\overline{\vartheta}^{HS}$ in (7). The expression $(1 - \sum_{i,j\in\Omega_h} \gamma^{HP}_{h,t}) \cdot \overline{\vartheta}^{HS}_{h,J}$ ensures that the HS temperature is however not falsely limited if the HP is inactive and thus activates the upper bound of $\overline{\vartheta}^{HS}_{h,J}$ which is the maximum temperature of the HS.

$$P^{HP}_{h,t} = \sum_{i,j\in\Omega_h} \left(\gamma^{HP}_{h,t,i,j} \cdot P^{fix}_{h,i}\right) \cdot \Gamma^{HP}_{h,t} \quad \forall \quad h \in H', t \in T^{HP} \tag{6}$$

$$\vartheta^{HS}_{h,t} \cdot \Gamma^{HP}_{h,t} \le \left(\sum_{i,j\in\Omega_h} \left(\gamma^{HP}_{h,t,i,j} \cdot \left(\overline{\vartheta}^{HS}_{h,j} + \vartheta^{amb}_{t}\right)\right) + \left(1 - \sum_{i,j\in\Omega_h} \gamma^{HP}_{h,t,i,j}\right) \cdot \overline{\vartheta}^{HS}_{h,J}\right) \cdot \Gamma^{HP}_{h,t} \quad \forall \quad h \in H', t \in T^{HP} \tag{7}$$

The heat flow $\dot{Q}^{H}$ that is directed from a HS to the corresponding household is limited with respect to the heat transfer coefficient kA in (8). However, the heating potential only increases up to a supply point maximum $\vartheta^{HP,sup}$ (9). ϑ^{H} denotes a household's temperature.

$$\dot{Q}^{H}_{h,t} \le \left(\vartheta^{HS}_{h,t} - \vartheta^{H}_{h,t}\right) \cdot kA_h \quad \forall \quad h \in H', t \in T^{HP} \tag{8}$$

$$\dot{Q}^{H}_{h,t} \le \left(\vartheta^{HP,sup}_{h} - \vartheta^{H}_{h,t}\right) \cdot kA_h \quad \forall \quad h \in H', t \in T^{HP} \tag{9}$$

The warm water demand $\dot{Q}^{w}$ is considered in (10). This demand can only be met by heat that is generated at a sufficiently high temperature. Consequently, this demand must be met by either HPs at operational modes with $i, j \in \Omega^{w}$ that only contain the respective intervals j, or by HRs with operating power P^{HR} which is limited in (11). The efficiency of HRs is given by η^{HR}.

$$\sum_{t\in T^{HP}} \left(\sum_{i,j\in\Omega^{w}_h} \left(\gamma^{HP}_{h,t,i,j} \cdot \dot{Q}^{fix}_{h,i,j}\right) + P^{HR}_{h,t} \cdot \eta^{HR}_{h} \right) \cdot \Pi^{HP} \ge \sum_{t\in T} \dot{Q}^{w}_{h,t} \quad \forall \quad h \in H' \tag{10}$$

$$P^{HR}_{h,t} \le \overline{P}^{HR}_{h} \quad \forall \quad h \in H', t \in T^{HP} \tag{11}$$

The temperatures in the households and in the HS are dynamically balanced taking into consideration all in- and outgoing heat flows in (12) and (13), respectively. In addition to the directly induced heat transfer into a household, heat dissipation and transmittance between household and HS, household and ambience, and through ventilation are taken into account in dependence of the thermal transmittance coefficients UA^{HS} and UA^{H} and the ventilation loss coefficient k^{vent}. The heat loss of the HRs' and TSLs' operating power and of the BSs' (dis-)charging power contribute according to the efficiency η. Furthermore, the impact of the base loads P^{L} and of solar irradiation $\dot{Q}^{sol}$ is considered. A household's thermal mass C^{H} determines the resulting thermal impact of the change in enthalpy. To take into account that the P2H systems are modeled in a broader time step width, the other components are summed over the intermediate time steps. Equations analogous to (12) and (13) are required for $t = 0$ with respective initialization values.

$$\begin{aligned}\vartheta^{H}_{h,t} = \vartheta^{H}_{h,t-\Delta t^{HP}} + \Bigg[&\Delta t^{HP} \cdot \Big(\dot{Q}^{H}_{h,t} + UA^{HS}_{h} \cdot \left(\vartheta^{HS}_{h,t} - \vartheta^{H}_{h,t}\right) \\ &- (\vartheta^{H}_{h,t} - \vartheta^{amb}_{h,t}) \cdot \left(UA^{H}_{h} + k^{vent}_{h,t}\right) + P^{HR}_{h,t} \cdot \left(1 - \eta^{HR}_{h}\right)\Big) \\ &+ \Delta t \cdot \sum_{t'=t}^{t+\Pi^{HP}-1} \Bigg(P^{L}_{h,t'} + \sum_{b\in B_h} \left(P^{BS,c}_{b,t'} + P^{BS,d}_{b,t'}\right) \cdot (1 - \eta^{BS}_{b}) + \dot{Q}^{sol}_{h,t'} \\ &+ \sum_{d\in D_h} P^{TSL}_{d,t'} \cdot \left(1 - \eta^{TSL}_{d}\right)\Bigg)\Bigg] \cdot \frac{1}{C^{H}_{h}} \quad \forall \quad h \in H', t \in T^{HP} \setminus \{0\}\end{aligned} \tag{12}$$

In addition to the heat flow from a P2H system, an HS receives heat from residential ST systems. An HS's enthalpy is converted into temperature through division by its heat capacity C^{HS}.

$$\begin{aligned}\vartheta^{HS}_{h,t} = \vartheta^{HS}_{h,t-\Delta t^{HP}} + \Bigg[&\Big(\dot{Q}^{HP}_{h,t} - \dot{Q}^{H}_{h,t} - UA^{HS}_{h} \cdot (\vartheta^{HS}_{h,t} - \vartheta^{H}_{h,t}) \\ &+ P^{HR}_{h,t} \cdot \eta^{HR}_{h}\Big) \cdot \Delta t^{HP} + \sum_{t'=t}^{t+\Pi^{HP}-1} \left(\dot{Q}^{ST}_{h,t'} - \dot{Q}^{w}_{h,t'}\right) \cdot \Delta t \Bigg] \cdot \frac{1}{C^{HS}_{h}} \\ &\forall \quad h \in H', t \in T^{HP} \setminus \{0\}\end{aligned} \tag{13}$$

The household temperature must further stay within lower and upper bounds for comfort (14). To ensure a higher level of comfort at which the bounds are not just minimally maintained, tighter bounds are defined in (15) that must be maintained on average over a comfort time window T^{c}.

$$\underline{\vartheta}^{H}_{h,t} \le \vartheta^{H}_{h,t} \le \overline{\vartheta}^{H}_{h,t} \quad \forall \quad h \in H', t \in T^{HP} \tag{14}$$

$$\underline{\vartheta}^{c}_{h} \le \sum_{t\in T^{c}} \vartheta^{H}_{h,t} \cdot \frac{1}{|T^{c}|} \le \overline{\vartheta}^{c}_{h} \quad \forall \quad h \in H' \tag{15}$$

In order to prevent minimization of the HS' state of charge (SOC) at the end of the planning period $\max(T^{HP})$, a defined temperature threshold $\vartheta^{HS,end}$ is set as a lower bound in (16). This threshold should be determined in accordance with forecasts for following planning periods.

$$\vartheta^{HS}_{h,\max(T^{HP})} \ge \vartheta^{HS,end}_{h} \quad \forall \quad h \in H' \tag{16}$$

3.3.2. Cooling mode

The operation of P2H systems in cooling mode features fundamental differences compared to their operation in heating mode. A parameter matrix P^{fix} is set up for intervals i of the heat flow $\dot{Q}^{HP}$ that is extracted from a household, and for intervals j of the difference between household temperature and a HP's cooling supply temperature ϑ^{cool}. Thus, the corresponding operating power is determined in (17) under consideration of the respective EER. Inequality (5) is required in the same way as in heating mode.

$$P^{HP}_{h,t} = \sum_{i,j\in\Omega_h} \left(\gamma^{HP}_{h,t,i,j} \cdot P^{fix}_{h,i,j}\right) \cdot \Gamma^{HP}_{h,t} \quad \forall \quad h \in H', t \in T^{HP} \tag{17}$$

The bounds for the resulting heat flow and temperature difference are set in (18) and (19), and (20), respectively. A sufficiently large temperature ϑ^{M} relaxes the bounds in the case of HP inactivity (20).

$$\dot{Q}^{HP}_{h,t} \leq \sum_{i,j\in\Omega_h} \left(\gamma^{HP}_{h,t,i,j} \cdot \overline{\dot{Q}}^{HP}_{h,i}\right) \cdot \Gamma^{HP}_{h,t} \quad \forall \quad h \in H', t \in T^{HP} \tag{18}$$

$$\dot{Q}^{HP}_{h,t} \geq \sum_{\substack{i,j\in\Omega_h\\ i\neq 0}} \left(\gamma^{HP}_{h,t,i,j} \cdot \overline{\dot{Q}}^{HP}_{h,i-1}\right) \cdot \Gamma^{HP}_{h,t} \quad \forall \quad h \in H', t \in T^{HP} \tag{19}$$

$$\begin{aligned}(\vartheta^{amb}_{t} - \vartheta^{cool}_{h,t}) \cdot \Gamma^{HP}_{h,t} \leq \Bigg(&\sum_{i,j\in\Omega_h} \left(\gamma^{HP}_{h,t,i,j} \cdot \overline{\vartheta}^{cool}_{j,h}\right) \\ &+ \Bigg(1 - \sum_{i,j\in\Omega_h} \gamma^{HP}_{h,t,i,j}\Bigg) \cdot \vartheta^{M} \Bigg) \cdot \Gamma^{HP}_{h,t} \\ &\forall \quad h \in H', t \in T^{HP}\end{aligned} \tag{20}$$

The heat flow $\dot{Q}^{HP}$ is determined by the difference between household temperature and cooling supply temperature and by the heat transfer coefficient kA^{cool} in (21). The positive buffer variable ϑ^{buff} prevents infeasibility in the case of household temperatures below the minimum cooling supply temperature. Since this is only relevant when a HP is not in operation, the buffer is only active in that instance. This is ensured in (22).

$$\dot{Q}^{HP}_{h,t} = \left(\vartheta^{H}_{h,t} - \vartheta^{cool}_{h,t} + \vartheta^{buff}_{h,t}\right) \cdot kA^{cool}_{h} \cdot \Gamma^{HP}_{h,t} \quad \forall \quad h \in H', t \in T^{HP} \tag{21}$$

$$\vartheta^{buff}_{h,t} \leq \vartheta^{M} \cdot \sum_{i,j\in\Omega_h} \gamma^{HP}_{h,t,i,j} \quad \forall \quad h \in H', t \in T^{HP} \tag{22}$$

Analogous to (12), the temporal temperature balance equation of households is considered in (23). For $t = 0$, (23) is to be formulated again with respective initialization values.

$$\begin{aligned}\vartheta^{H}_{h,t} = \vartheta^{H}_{h,t-\Delta t^{HP}} + \Bigg[&\Delta t^{HP} \cdot \left(-\dot{Q}^{HP}_{h,t} - (\vartheta^{H}_{h,t} - \vartheta^{amb}_{t}) \cdot \left(UA^{H}_{h} + k^{vent}_{h,t}\right)\right) \\ &+ \Delta t \cdot \sum_{t'=t}^{t+\Pi^{HP}-1} \Bigg(P^{L}_{h,t'} + \sum_{b\in B_h} (P^{BS,c}_{b,t'} + P^{BS,d}_{b,t'}) \cdot (1 - \eta^{BS}_{b}) + \dot{Q}^{sol}_{h,t'} \\ &+ \sum_{d\in D_h} P^{TSL}_{h,t'} \cdot (1 - \eta^{TSL}_{d})\Bigg)\Bigg] \cdot \frac{1}{C^{H}_{h}} \\ &\forall \quad h \in H', t \in T^{HP} \setminus \{0\}\end{aligned} \tag{23}$$

Analogous to (10) and (11), the warm water demand is considered in (24). However, in cooling mode only HRs and the heat provided by ST systems are available for this purpose.

$$\sum_{t\in T^{HP}} \left(P^{HR}_{h,t} \cdot \eta^{HR}_{h}\right) \cdot \Pi^{HP} \geq \sum_{t\in T} \dot{Q}^{w}_{h,t} - \dot{Q}^{ST}_{h,t} \quad \forall \quad h \in H' \tag{24}$$

Constraint groups (14) and (15) are also required in cooling mode.

3.4. Electric vehicles and battery storage systems

The scheduling of the set of EVs N considers individual driving profiles that specify the time windows and energy consumption for the driving demand of individual EVs, and which are assumed to be known. Accordingly, each EVs has a limited temporal availability T^{EV} for (dis-)charging and for using it as a flexible energy storage only when it is not driven. Thus, in the case of unavailability, the (dis-)charging power P is limited to zero in (25). For $t \in T^{EV}$, the upper bounds $\overline{P}^{EV}$ are activated by binary variables γ that determine whether EVs are in charging or discharging mode (26 and 27), only one of which can be active at a time (28).

$$P^{EV,c}_{n,t}, P^{EV,d}_{n,t} \leq 0 \quad \forall \quad n \in N, t \in T \setminus T^{EV}_{n} \tag{25}$$

$$P^{EV,c}_{n,t} \leq \overline{P}^{EV}_{n} \cdot \gamma^{EV,c}_{n,t} \quad \forall \quad n \in N, t \in T^{EV}_{n} \tag{26}$$

$$P^{EV,d}_{n,t} \leq \overline{P}^{EV}_{n} \cdot \gamma^{EV,d}_{n,t} \quad \forall \quad n \in N, t \in T^{EV}_{n} \tag{27}$$

$$\gamma^{EV,c}_{n,t} + \gamma^{EV,d}_{n,t} \leq 1 \quad \forall \quad n \in N, t \in T^{EV}_{n} \tag{28}$$

The (absolute) SOC is modeled over time, taking into account (dis-)charging with efficiency η and the required SOC according to the driving profiles in (29). The efficiency is only considered for charging, but not for discharging, as $P^{EV,c}$ and $P^{EV,d}$ are defined as the ideal, loss-free power. Due to losses, less than the ideal power contributes to the SOC of an EV when it is charged, whereas the efficiency losses only affect the power which is made available to a household by discharging an EV. The consideration of the discharging efficiency consequently occurs in the household power balance (38), and not in constraint (29). To account for a sufficiently high SOC at the beginning of a driving period and, simultaneously, for a reduced SOC after a driving period, the respective amount is considered as a consumption (represented by $SOC^{EV,req}$) in the last time step before a driving period; this is a parameter resulting from the driving profile. An analogous equation for $t = 0$ is required with respective initialization values.

$$\begin{aligned}SOC^{EV}_{n,t} = SOC^{EV}_{n,t-1} &+ \left(P^{EV,c}_{n,t} \cdot \eta^{EV}_{n} - P^{EV,d}_{n,t}\right) \cdot \Delta t \\ &- SOC^{EV,req}_{n,t+1} \quad \forall \quad n \in N, t \in T^{EV}_{n} \setminus \{0\}\end{aligned} \tag{29}$$

Upper and lower bounds for the SOC ($\overline{SOC}^{EV}$ and $\underline{SOC}^{EV}$) are defined in (30) and (31). The binary variable in (31) ensures that the lower bound may not be surpassed by discharging, which is only the case if the binary variable $\gamma^{EV,d}$ is assigned a value of one.

$$SOC^{EV}_{n,t} \leq \overline{SOC}^{EV}_{n} \quad \forall \quad n \in N, t \in T^{EV}_{n} \tag{30}$$

$$SOC^{EV}_{n,t} \geq \underline{SOC}^{EV}_{n} \cdot \gamma^{EV,d}_{n,t} \quad \forall \quad n \in N, t \in T^{EV}_{n} \tag{31}$$

Analogous to (16), a lower bound SOC^{end} for the SOC at the end of the planning period T is be defined in (32). This accounts for a foresighted planning approach as it prevents storages from being emptied at the end of the planning period.

$$SOC^{EV}_{n,\max(T^{EV}_{n})} \geq SOC^{end}_{n} \quad \forall \quad n \in N \tag{32}$$

The set B of BSs is modeled with constraints analagous to (25) to (30) and (32), but without limited temporal availability and without $SOC^{BS,req}$, as no own demand is to be considered.

3.5. Time-shiftable loads

TSLs are represented by set D. Each TSL has an available time window T^{TSL} in which a sequence of operational phases T^{τ} with respective power p^{TSL} needs to be scheduled. The binary variable γ^{TSL} in (33) determines which phase is active at which time. Thus, the power variable P^{TSL} is assigned the respective value of p^{TSL}. For reasons of efficiency, only operational phases τ that are not greater than the position of t in T^{TSL} are considered (e.g. the second operational phase cannot be active in the first time step).

$$P^{TSL}_{d,t} = \sum_{\substack{\tau \in T^{\tau}_d \\ \tau \le pos(t, T^{TSL}_d)}} p^{TSL}_{d,\tau} \cdot \gamma^{TSL}_{d,t,\tau} \quad \forall \quad d \in D, t \in T^{TSL}_d \tag{33}$$

The set $T^{start}_d \subseteq T^{TSL}_d$ contains the time steps in which the operation of d may be started. Eq. (34) ensures that the starting phases with $\tau = 0$ are activated exactly once. Starting the operation at any time after the starting time window is prevented by (35).

$$\sum_{t \in T^{start}_d} \gamma^{TSL}_{d,t,0} = 1 \quad \forall \quad d \in D \tag{34}$$

$$\sum_{t \in T^{TSL}_d \setminus T^{start}_d} \gamma^{TSL}_{d,t,0} \le 0 \quad \forall \quad d \in D \tag{35}$$

Eq. (36) maintains the uninterrupted sequence of operational phases. The sets T'^{TSL} and T'^{τ} represent T^{TSL} and T^{τ} without the respective first value of the set, as there are no predecessors defined for the first time step and first operational phase.

$$\gamma^{TSL}_{d,t,\tau} = \gamma^{TSL}_{d,t-1,\tau-1} \quad \forall \quad d \in D, t \in T'^{TSL}_d, \tau \in T'^{\tau}_d \tag{36}$$

To prevent the operation of TSLs outside of the time window T^{TSL}, (37) is required.

$$P^{TSL}_{d,t} \le 0 \quad \forall \quad d \in D, t \in T \setminus T^{TSL}_d \tag{37}$$

3.6. Balance and trading constraints

The scheduling of DERs has to take into account that each household's energy supply and demand must be balanced at all times. The balance equation with the power of all DERs and trading variables is modeled in (38). Regarding EVs and BSs, the efficiency η is only considered in the case of discharging, as the charging losses do not contribute to the household power balance.

$$\begin{aligned}
&\sum_{b \in B_h} \left(P^{BS,c}_{b,t} - P^{BS,d}_{b,t} \cdot \eta^{BS}_b \right) + \sum_{n \in N_h} \left(P^{EV,c}_{n,t} - P^{EV,d}_{n,t} \cdot \eta^{EV}_n \right) \\
&+ \sum_{d \in D_h} P^{TSL}_{d,t} + P^{L}_{h,t} + P^{HP}_{h,t} + P^{HR}_{h,t} = P^{PV}_{h,t} \\
&+ P^{WS,buy}_{h,t} - P^{WS,sell}_{h,t} + \left(P^{LM,buy}_{h,t} - P^{LM,sell}_{h,t} \right) \cdot \Lambda^{LM}_t \\
&+ \left(P^{int,buy}_{h,t} - P^{int,sell}_{h,t} \right) \cdot \Lambda^{int}_t \quad \forall \quad h \in H, t \in T
\end{aligned} \tag{38}$$

Furthermore, each household is limited to either purchasing or selling at a specific time step (39). A sufficiently large P^M is activated as an upper bound for trading if the respective binary variable γ^{buy} or γ^{sell} assumes a value of 1 in (40) and (41).

$$\gamma^{buy}_{h,t} + \gamma^{sell}_{h,t} \le 1 \quad \forall \quad h \in H, t \in T \tag{39}$$

$$\begin{aligned}
&P^{WS,buy}_{h,t} + P^{LM,buy}_{h,t} \cdot \Lambda^{LM}_t + P^{int,buy}_{h,t} \cdot \Lambda^{int}_t \le \gamma^{buy}_{h,t} \cdot P^M \\
&\forall \quad h \in H, t \in T
\end{aligned} \tag{40}$$

$$\begin{aligned}
&P^{WS,sell}_{h,t} + P^{LM,sell}_{h,t} \cdot \Lambda^{LM}_t + P^{int,sell}_{h,t} \cdot \Lambda^{int}_t \le \gamma^{sell}_{h,t} \cdot P^M \\
&\forall \quad h \in H, t \in T
\end{aligned} \tag{41}$$

For internal trading, the balance condition in (42) has to be fulfilled as internal trading is only possible if a purchaser and seller are matched.

$$\sum_{h \in H} P^{int,buy}_{h,t} \cdot \Lambda^{int}_t = \sum_{h \in H} P^{int,sell}_{h,t} \cdot \Lambda^{int}_t \quad \forall \quad t \in T \tag{42}$$

4. Case study

The EAM is applied in a case study of a network on distribution grid level with 111 prosumer households, the data for which originates from the SimBench data sets [44]. Each household has unique characteristics regarding the relevant parameters for the thermodynamic relations, and unique sets of DERs with individual characteristics. All parameters are configured in line with existing norms and regulations [45,46]. Each household is modeled with an HP. 94 of the 111 households are equipped with a PV system with peak powers in the range of 5.7 to 31.6 kW. 44 households have ST systems with maximum heat flow rates of 0.8–4.7 kW. Furthermore, 76 BSs are included. The respective capacities range from 2.4 to 14.4 kWh with a maximum power of 6 kW. The 111 households own a total of 140 EVs. Of the 94 households owning EVs, 54 own exactly one, 34 own two and 6 own 3 EVs. Technical data for the four types of considered models is presented in Table 1. Standardized load profiles from WPuQ data sets are applied to the households with individual scaling factors in accordance with the household area sizes [51]. Household sizes range from 96 to 533 square meters of living area.

Further parameters regarding environmental aspects such as solar radiation, ambient temperatures, WS energy prices and fees, as well as the load profiles are based on real data from the year 2019. Weather data is acquired from the German city of Hamelin [52]. The WS prices for the respective dates and times are taken from the European Energy Exchange (EEX) in Germany [53]. The LM prices are determined on the basis of WS prices as well as local demand and supply of energy in a way that incentives for local trading are created, both on purchaser and seller sides. Consumer fees are set in accordance with German regulations [54]. To account for the different operational modes of HPs, the case study is considered in two scenarios: a summer scenario, consisting of 62 individual summer days (cooling mode), and 62 individual winter days (heating mode) as a winter scenario. Each day represents a model instance as a single day-ahead optimization. The EAM is applied with a time step width of 30 min, overall, and 60 min for the operation of HPs.

In order to perform differentiated analyses, four different configurations of EAs are considered in the case study, in which the availability of trading levels is varied. In configuration C1, all three trading options are fully available, thus representing fully operational EAs in the way introduced above. In C2–C4, the availability of trading options is gradually decreased. In C2, internal trading is disabled, leaving only the options of trading on LM and WS level. In C3, only WS trading remains. The base case C4 represents an approximation of unaggregated and self-managing households that can only trade at prices that are fixed over the course of the whole day, thereby leaving no temporal price fluctuations to exploit. C4 can thus be viewed as a baseline for assessing the potential of EA, as it reflects the situation of single households without EAs.

Table 1
EV data [47–50].

Model name	Battery capacity	(Dis-)charging power limit
Tesla Model S Performance	100 kWh	16.5 kW
Volkswagen ID.4 Pro 4MOTION	82 kWh	11 kW
Volkswagen e-Up!	36.8 kWh	7.2 kW
Renault Zoe ZE40 R110	54.7 kWh	22 kW

The model instances resulting from the case study application are solved using Gurobi version 11 on a standard office workstation.

5. Results and discussion

In this section, the results from the two case study scenarios are presented and discussed. In order to validate the EAM's efficacy, the economic efficiency of EAs is analyzed, which is then further examined with respect to the different DER types.

5.1. EA efficiency

To analyze the economic efficiency of EA, the results regarding configurations C1 to C4 are presented and discussed in this subsection for both scenarios.

5.1.1. Summer scenario - cooling mode

One major characteristic of the summer scenario is that households with PV systems are at times provided with abundant energy. Accordingly, the amount of solar radiation on a specific day significantly influences the decisions and the economic potential of a local EA. This is illustrated in the graphs for all four configurations in Fig. 3 which show that the daily household average trading profit for the 111 aggregated households significantly increases with increasing solar radiation ($R^2 = 0.810$ for C1).

Although all four configurations are subject to the aforementioned positive relationship between solar radiation and profit, the regression lines reveal a clear hierarchy regarding profitability. Whereas households in the baseline configuration C4 make average daily profits of only 1.54 €, enabling the exploitation of WS price fluctuations in C3 provides them with a profit increase of 2.04 € or 132.24 % on average in comparison to C4. The LM further adds 1.14 € in C2, and in C1 the average daily household profit is again increased by 0.22 €. In relation to C4 this adds up to a difference of 3.4 € or 220.15 %. In the C4 graph, a nearly linear relationship between profit and solar radiation is observed. This indicates that with more solar radiation, there is more energy available to be sold for a fixed price and thus, the marginal profit is nearly constant. In the absence of variable prices and other trading options, there are no notable opportunities to utilize abundant energy more efficiently. Since households are not interconnected by internal trade, the only alternative for using abundant energy is by the resident households themselves. The profit differences between the configurations increase with increasing solar radiation. A higher degree of flexibility thus enables synergy potentials to be exploited. Even without internal and local trading, flexible WS prices (C3) provide large benefits by enabling abundant energy to be sold at times of high prices. The resident households' flexibility allows them to store energy until the most beneficial times. In C2, enabling the EA to also trade on LM level gives further options for profitably selling abundant energy, increasing the gap between C2 and C3 even more with increasing solar radiation. Additionally, profits can be slightly increased even more with internal trading, as direct synergies between households are realized. The largest gap can, however, be observed between C3 and C4, i.e. flexible WS prices comprise the highest potential for optimization. This relates to the limited trading opportunities on LM and internal levels due to small numbers of market participants, especially under influence of locally homogeneous phenomena such as solar radiation and their impact on local prices. As a consequence, the majority of trading is done on WS level. An illustration is provided in Fig. 4, which shows the proportions of trading volumes on the three different trading levels in dependence on the daily total solar radiation for each of the 62 days from the case study, respectively.

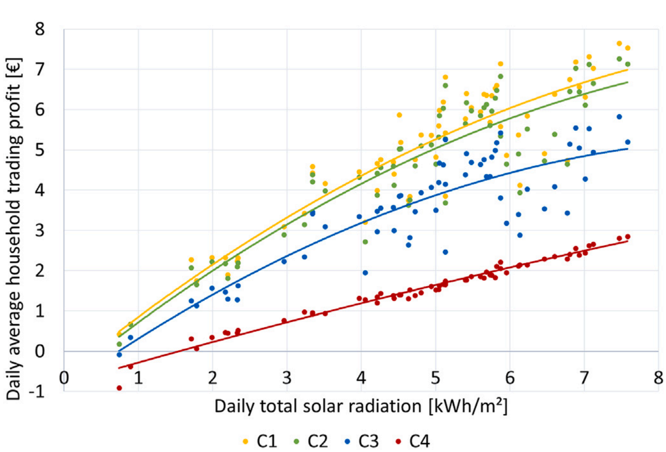

Fig. 3. Summer scenario results.

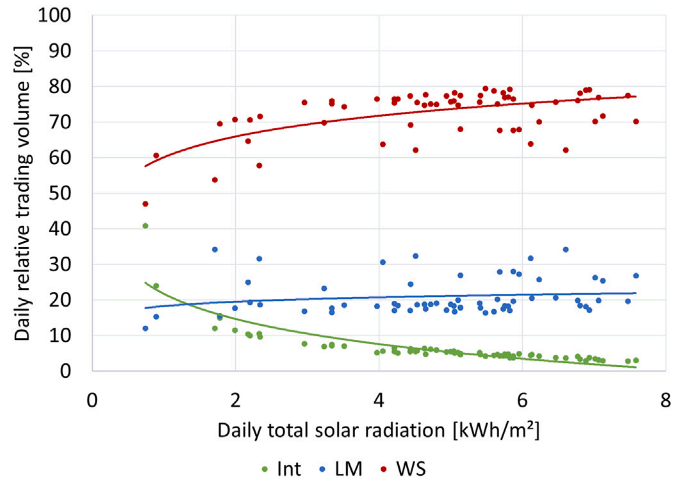

Fig. 4. Summer scenario relative trading volumes (C1).

A notable difference is also visible between the potential of local compared to internal trading, as the gap between C2 and C3 is significantly larger than the gap between C1 and C2. This is partly due to the overall higher trading volume on LM level. Furthermore, the inherent nature of internal trading limits it to relatively small profit margins compared to external trading options. Internal trading between two households can only be initiated if both participants have a monetary incentive and this is only the case if the respective WS and LM prices are sufficiently close to each other. Otherwise, for either the purchaser or the seller an external trading option would be more profitable and an internal trade would not take place. Larger differences between the external prices not only disable internal trading, but also enable more profitable options for exploiting extreme prices. Specifically, internal trading is only enabled if the sum of the higher external price and the internal trading fee is lower than the sum of the lower external price and the respective external fee. The degree to which internal trading is subsidized with low fees, is therefore a factor that can improve availability and profitability of internal trading.

The above results validate the efficacy of the EAM, as the economic potential of multiple trading options and locally abundant energy is exploited. The advantage of a holistic approach considering multiple trading options is thus shown as the opportunities to monetize these options result from the interdependence of trading and flexibly scheduling various DERs. Before assessing the contribution of different flexibility types to these profit gains, analogous analyses are performed for the winter scenario.

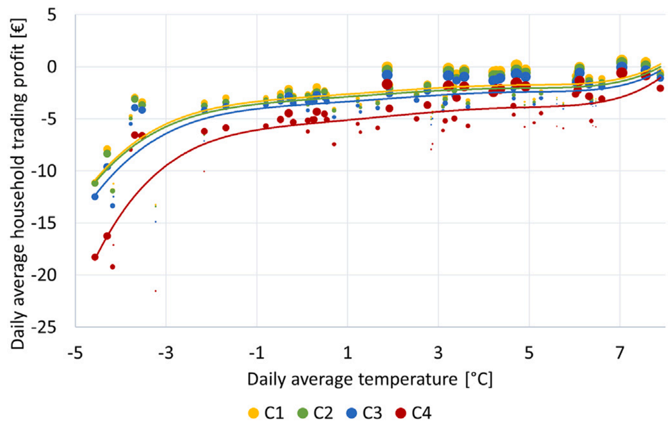

Fig. 5. Winter scenario results (bubble size indicates solar radiation).

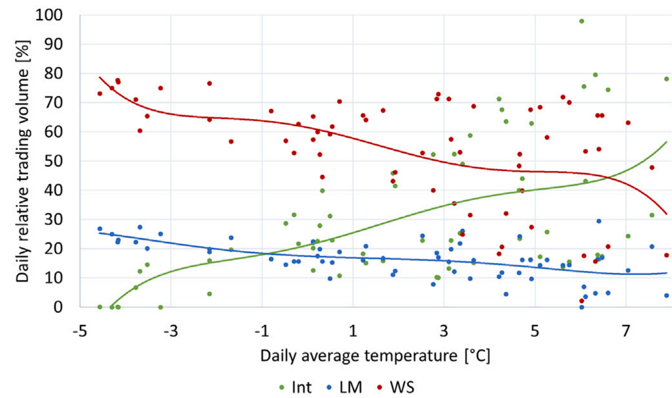

Fig. 6. Winter scenario relative trading volumes (C1).

5.1.2. Winter scenario – heating mode

The characteristics of the winter scenario have two major differences in regard to the summer scenario. The households' loads, especially heating loads, are higher, and there is only little PV-generated energy. Both aspects negatively influence the trading profit. Contrary to summer days, the households on average record losses on the vast majority of days due to the necessity of purchasing and little potential for selling energy. Although the profit is more strongly correlated with the daily average temperature ($R^2 = 0.465$ for C1) than with the amount of solar radiation ($R^2 = 0.331$ for C1), the impact of both factors is visible in Fig. 5. Due to increased computation times for the more complex heating mode, the results in this scenario are based on an EAs with only 10 households.

Low temperatures lead to increasing costs due to additional heating loads, whereas higher amounts of solar radiation reduce the losses, or even enable slight profits on warmer days. The hierarchy of configurations C1 to C4 is equivalent to the summer scenario. Whereas self-managing households in C4 have daily trading deficits of 5.70 € on average to cover their loads, this is reduced by 1.99 € (34.93 %) in C3. Enabling further trading options in C2 and C1 additionally reduces the average daily trading losses by 0.49 € (13.19 %) and 0.27 € (8.33 %), respectively. In relation to the baseline C4, an EA in C1 reduces the overall household energy cost by 2.75 € or 48.22 % on average per day. These findings show that the highest potential for optimization lies in minimizing the purchasing costs on WS level which is the overall dominant trading option. A more differentiated analysis in Fig. 6 reveals that the proportion of internal trading increases with increasing temperature and eventually exceeds the proportion of WS trading. On cold days a lot of energy is bought externally to cover high heating demands. The low internal trading volumes at the same time indicate that due to high resident loads, few flexibility options are left to be exploited. Despite the overall trading volume on LM level being lower than the internal trading volume, the profit gap between C3 and C2 is relatively larger than the one between C2 and C1, i.e. local trading contributes more to profit gains than internal trading due to higher profit margins on this level. The gap between C1 and C2 converges towards zero for cold days which is evident considering that nearly no internal trading occurs on these days (see Fig. 6).

In line with the summer scenario results, the efficacy of the EAM is also validated for the winter scenario, as the different trading options are exploited to the benefit of participating households, thereby supporting the holistic approach. All three trading options provide benefits that, however, strongly differ within the days analyzed in the case study. Only due to the explicit modeling of the interdependence between energy trading and DER scheduling, the analyzed effects can be taken into account and the potential of EAs can be exploited.

5.2. Flexibility type analysis

To gain deeper insights into the above results, a closer look at the interrelations between the scheduling of DERs and economic efficiency is taken in this section with the aim of assessing whether the integration and detailed consideration of the respective DER types into the EAM are beneficial.

5.2.1. Power-to-heat systems

The impact of the P2H operation differs significantly between seasonal scenarios. In the summer scenario, the heating load constantly constitutes about 12 % of the daily total load for all four EA configurations. The impact of cooling is negligibly small, as the HPs are barely in operation on most days under the moderate conditions of a German summer with daily average temperatures in the range of 13 °C–25 °C. On the hottest days in the case study with average temperatures of up to 28 °C, the average household cooling load reaches at most 0.34 kWh of electrical power. This is still very low in comparison to the warm water (WW) demand, which requires between 3 and 5 kWh for HR operation. Two conclusions regarding the modeling of P2H systems can be drawn: a detailed consideration of a HP's cooling mode might only be useful under more extreme weather conditions that require more cooling; and since the WW demand also has to be covered on warm days, this heating load could be provided by HPs rather than HRs more efficiently by also integrating the heating mode in the summer scenario.

A major cause of the massive increase in losses on cold winter days, observed in Fig. 5, can be found within the operation of P2H systems. As can be seen in Fig. 7, the heating load covered by HPs increases with decreasing temperature, i.e. with increasing heating demand. This plausible relation is only disrupted on the coldest days in the case study with average temperatures of less than −3 °C which show a reduction in the operation of HPs. Since they cannot be operated at ambient temperatures below the bivalence point of −5 °C, at these times HPs are replaced by HRs as heat sources. Due to the low efficiency of HRs, they require comparatively higher operational power to substitute HPs, resulting in overall higher heating loads. On days that are not affected by the bivalence point, the operation of HR is limited to negligibly small loads. The strong impact of overall heating load on trading profit in the winter scenario is underlined by an R^2 value of 0.792 for C1.

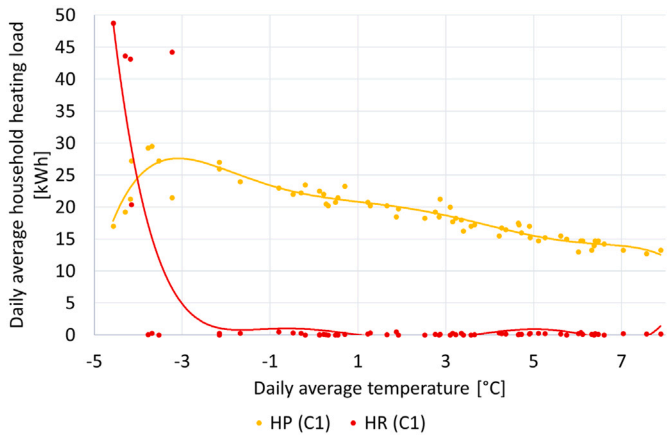

Fig. 7. Winter scenario P2H operation (C1).

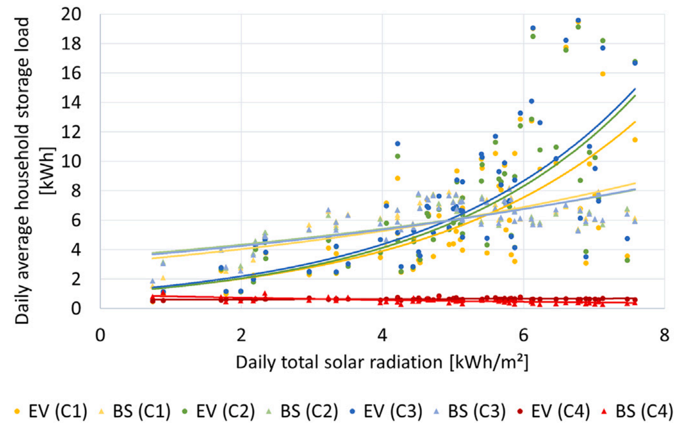

Fig. 8. EVs and BSs charging in the summer scenario.

In order to provide an adequate basis for the operational decisions of P2H systems and considering the inherent complex efficiency factors that have significant impact on economic efficiency, it is necessary to model these systems with a high level of detail. Without adequately modeling such thermal aspects, optimization results are prone to stronger efficiency deviations compared to the real-world operation of P2H systems. Accordingly, the operational times of HPs are non-trivially scattered over the course of days, dependent not only on energy prices but also on the availability of abundant or stored energy at the respective households. The different operating modes come into play and significantly influence the overall efficiency as the corresponding COPs assume values in the range of 2.3018 to 4.0208, depending on the respective ambient temperatures and heat storage temperatures over the course of a day. Assuming a constant COP and not accounting for the specific heat flows in the households would have a strong impact on the heating loads depicted in Fig. 7 and provide unrealistic results, as significant fluctuations in efficiency would be neglected.

The above findings furthermore suggest that it might provide additional optimization potential to take weather forecasts for following days into account so that HSs can be efficiently filled by HPs on moderately cold days that are followed by colder days with restricted operation of HPs. Whereas this has the drawback of increased computational effort, the observed effects of efficiently deploying HPs can be expected to have even higher potential over a time horizon of more than one day.

5.2.2. Energy storages

It can be expected that the shown results are intertwined with the utility of energy storage in BSs and EVs. An overview of the respective charging loads is presented in Fig. 8 for C1–C4 in the summer scenario. Significant qualitative differences can be observed between the four EA configurations. In C4, the storage capacities are used only to a marginal extent of less than 1 kWh per household. This indicates that these resources are only charged when the respective household can use abundant energy at a later time of day. If the prices are constant over time, there is no potential for strategically deploying storage at convenient times. Whereas the charging load of EVs is nearly constant for all instances in the case study, there is a slightly negative relation between solar radiation and BSs usage. Although more solar radiation provides more energy overall, simultaneously the demand for purchasing energy decreases as many households have an abundance of energy themselves, thereby also decreasing the overall need for storing energy for later use. Days with less solar radiation and, thus, shorter time periods of energy abundance consequently exhibit more opportunities for using stored energy at a later time.

For both storage types, the usage is nearly identical in C3 and C2. This indicates that nearly no synergies are realized between storage flexibility and LM trading. However, with increasing solar radiation there is an increase in storage loads. By exploiting flexible WS prices, abundant energy can be stored beneficially to be sold at times of high prices. A qualitative difference is observable between EVs and BSs: whereas BSs are the dominant storage type on days with low solar radiation, the usage of EVs increases more strongly with increasing abundance of energy. Contrarily, on sunny days significantly more energy is stored in EVs than in BSs. When energy is scarce, the unlimited temporal flexibility of BSs provides an advantage for more efficient use. With increasing abundance of energy, constraints of lower capacities and charging power limits become more restrictive. In C1, there is only a marginal difference in the usage of BSs in comparison to C2 and C3. The amount of energy stored in EVs increases with increasing solar radiation, but to a lesser extent than in C2 and C3. This shows that occasionally it is more beneficial to trade abundant energy internally instead of storing it for own use or for externally selling at a later time. Although in these instances the overall amount of internal trading is low (see Fig. 4), exactly these internal trades substitute the usage of storages. This shows that demands of households without PV systems and without resident abundant energy can be covered more efficiently through internal trading.

Contrary to the summer scenario, in the winter scenario (see Fig. 9) BSs are the dominant storage type, whereas the flexibility of EVs is only used to a small extent of one to three kWh of stored energy as the household average per day. The differences between C1, C2 and C3 in regard to EVs usage are marginal, only in C4 a slight decrease is observable. This shows that the impact of EVs storage flexibility is minor due to the temporal restrictions of use. In contrast to summer days, during which energy storage systems are used to store vast amounts of abundant solar energy at once, on winter days the flexibility of purchasing energy at times of low prices and consuming it at times of high demand is more important than high capacities and (dis-)charging powers of storages. The usage of BSs is subject to a strong increase on the coldest winter days as there are higher heating demands to be covered (see Fig. 7). The above findings underline the significant impact of the storage parameters temporal availability, (dis-)charging power and capacity. The limited deployment of EVs flexibility in the winter scenario leads to the conclusion that frequent communication between households and EAs regarding the planned or estimated usage of EVs is a

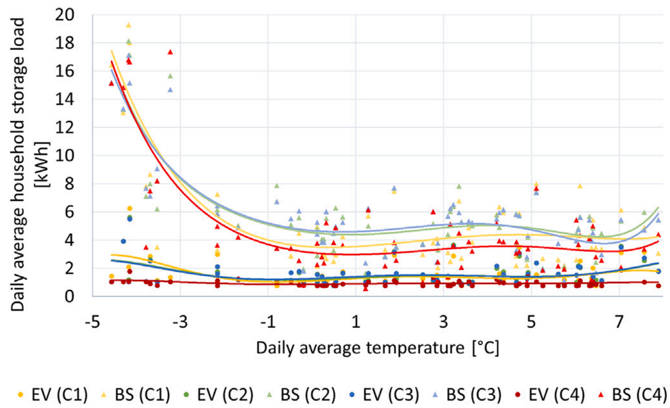

Fig. 9. EVs and BSs charging in the winter scenario.

critical aspect for realizing the inherent potential because high availability is an important factor for efficiently utilizing the flexibility of EVs. On the other hand, the efficiency potential of BSs is limited by the maximum charging power of 6 kW and could be increased with more powerful energy storages. The complexity within the above findings supports the necessity of holistically considering different energy storages in combination with the unique properties of other DERs in order to take the inherent interrelations into account. As different properties of storages result in different usage patterns, the economic potential of energy storages can be seen to strongly depend on various other factors. This includes external factors such as solar radiation or ambient temperature, as well as other sources of flexibility to generate synergies within interdependent scheduling decisions. Thus, an adequate consideration of these interrelations in the model by holistically integrating different types of flexible DERs and multiple trading options is necessary to exploit the inherent potential. This work contributes to research by developing a respective EAM that takes these interdependencies into account in a differentiated way.

6. Conclusion

In this work, a MILP model for the day-ahead EA problem is introduced as a base model that holistically integrates all major aspects of the operation of such a system. Decisions regarding multiple different trading options, including internal trading between households of the same EA and thereby forming an EC, are integrated into the operational decision making regarding the deployment of different types of DERs with their respective technological properties. A special contribution to existing work on EA optimization lies in the high level of detail in the modeling of P2H systems with HPs to enable coupling of the electrical and thermal systems. The model is applied to a case study consisting of a summer and a winter scenario with 62 days, respectively, and real weather and energy price data for these days. In the summer scenario, an EA with 111 individually modeled prosumer households is considered, whereas the study is limited to 10 households in the winter scenario due to high computation times. The results reveal high potential for realizing trading profits on behalf of the aggregated households that can be attributed to the different system components and synergies between them. Thus, the efficacy of the model is validated, underlining the importance of a holistic approach with a high level of detail that enables an explicit consideration of these synergies. In both scenarios, each of the three trading options (WS, LM and internal trading) significantly contributes to increasing profits. The inherent flexibility of DERs such as P2H systems, EVs, BSs and TSLs in combination with resident PV systems enables the exploitation of temporal fluctuations in energy prices. Although the overall impact of internal trading is lower in comparison to the other trading levels, it can be shown to provide profit increases of up to 10 % daily as the household average. Since this result is likely to be sensitive to the degree to which internal trading is monetarily incentivised in the form of reduced trading fees, future research regarding the impact of the structure of energy prices and fees on the economic efficiency of EAs could provide deeper insights into the potential of internal and local trading. A high level of detail regarding technological properties of different types of DERs has been shown to be useful in the context of EA operational decisions, as the potential of EAs is built on interdependent, synergistic effects between the different system components, and because these effects are not properly taken into consideration if the underlying technological details are neglected. In the winter scenario, efficiently covering the required heating loads is the major influencing factor of trading profit. The EAM provides a differentiated consideration of the thermal relations that allows an adequately realistic integration of P2H systems and, thus, additional synergetic potential. More potential in this regard could be raised by extending the planning horizon to consider subsequent days in the day-ahead optimization. In the summer scenario, profit is predominantly influenced by efficiently using abundant PV energy, which is fostered by usage of storage flexibility. An interesting finding is the trade-off between the temporal flexibility of storage systems and their charging power and capacity. Whereas in the summer scenario, EVs are dominantly used to store large amounts of abundant PV energy at high charging rates, the temporally unlimited flexibility of BSs is more beneficial in the winter scenario and on the less sunny summer days to exploit the full synergetic potential of energy price fluctuations, heating flexibility and internal trading.

The limitations of high computation times due to the high level of detail in modeling the EA problem provide future research opportunities for more efficient solution methods. As the concept of flexibility procurement for system operators is not considered in this work, a point of interest for future research on EAs could be an assessment of the potential for providing such ancillary services to grid operators by integrating this aspect into the EAM. Furthermore, performing in-depth analyses regarding the potential of a more foresighted deployment of energy storages and the influence of different energy price structures could diminish the limitations of this work resulting from simplified assumptions in regard to these aspects. Moreover, variable bidding prices on the energy markets could also be considered as a subject of optimization to account for a more realistic trading behavior.

CRediT authorship contribution statement

Kai Hoth: Writing – original draft, Visualization, Validation, Software, Methodology, Formal analysis, Data curation, Conceptualization. **Béla Wiegel:** Writing – review & editing, Validation, Methodology, Investigation, Data curation. **Tizian Schug:** Writing – review & editing, Visualization, Validation, Investigation, Conceptualization. **Kathrin Fischer:** Writing – review & editing, Validation, Supervision, Resources, Investigation, Funding acquisition, Conceptualization.

Declaration of competing interest

The authors declare that they have no known competing financial interests or personal relationships that could have appeared to influence the work reported in this paper.

Acknowledgment

The authors gratefully acknowledge financial support from the Ministry for Science, Research, Equality and Districts Authority, Hamburg, Germany.

Appendix

See Tables 2–4.

Table 2
Definition of sets.

Symbol	Definition
B	Set of BSs
B_h	Set of BSs of a household h
D	Set of TSLs
D_h	Set of TSLs of a household h
H	Set of households
H'	Set of households with a P2H system
N	Set of EVs
N_h	Set of EVs of a household h
T	Set of time steps
T^c	Set of time steps of comfort time window
T_n^{EV}	Set of time steps in which EV n is available
T^{HP}	Set of time steps for P2H system operational decisions
T_d^{start}	Set of time steps in which TSL d can be started
T_d^{TSL}	Set of time steps in which TSL d is available
$T_d^{\prime TSL}$	Set of time steps in which TSL d is available, excluding the first one
T_d^{τ}	Set of operational phases of TSL d
$T_d^{\prime\tau}$	Set of operational phases of TSL d, excluding the first one
Ω_h	Set of operational modes of HPs
Ω_h^{w}	Set of operational modes of HPs capable of covering warm water demand

Table 3
Definition of variables.

Symbol	Definition
$P_{b,t}^{BS,c}$	Charging power of a BS b
$P_{b,t}^{BS,d}$	Discharging power of a BS b
$P_{n,t}^{EV,c}$	Charging power of a EV n
$P_{n,t}^{EV,d}$	Discharging power of a EV n
$P_{h,t}^{HP}$	Operational power of a HP
$P_{h,t}^{HR}$	Operational power of a HR
$P_{h,t}^{int,buy}$	Power purchased on internal level
$P_{h,t}^{int,sell}$	Power sold on internal level
$P_{h,t}^{LM,buy}$	Power purchased on LM level
$P_{h,t}^{LM,sell}$	Power sold on LM level
$P_{d,t}^{TSL}$	Operational power of a TSL d
$P_{h,t}^{WS,buy}$	Power purchased on WS level
$P_{h,t}^{WS,sell}$	Power sold on WS level
$\dot{Q}_{h,t}^{H}$	Heat flow directed into a household
$\dot{Q}_{h,t}^{HP}$	Heat flow generated by a HP
$SOC_{b,t}^{BS}$	SOC of BS b
$SOC_{n,t}^{EV}$	SOC of EV n
$\gamma_{b,t}^{BS,c}$	Binary variable to (de-)activate charging of BS b
$\gamma_{b,t}^{BS,d}$	Binary variable to (de-)activate discharging of BS b
$\gamma_{h,t}^{buy}$	Binary variable to (de-)activate purchasing of energy
$\gamma_{n,t}^{EV,c}$	Binary variable to (de-)activate charging of EV n
$\gamma_{n,t}^{EV,d}$	Binary variable to (de-)activate discharging of EV n
$\gamma_{h,t,i,j}^{HP}$	Binary variable to (de-)activate operational mode i,j of a HP
$\gamma_{h,t}^{sell}$	Binary variable to (de-)activate selling of energy
$\gamma_{d,t,\tau}^{TSL}$	Binary variable to (de-)activate operational phase τ of TSL d
$\vartheta_{h,t}^{buff}$	Buffer variable for the cooling supply temperature of a HP
$\vartheta_{h,t}^{cool}$	Cooling supply temperature of a HP
$\vartheta_{h,t}^{H}$	Household temperature
$\vartheta_{h,t}^{HS}$	HS temperature

Table 4
Definition of parameters.

Symbol	Definition
C_h^{H}	Thermal mass of a household
C_h^{HS}	Heat capacity of a HS
f^{int}	Internal energy trading fee
f^{LM}	LM energy trading fee
f^{WS}	WS energy trading fee
k_h^{vent}	Ventilation loss coefficient
kA_h	Heat transfer coefficient
kA_h^{cool}	Cooling heat transfer coefficient
$P_{h,i}^{fix}$	Operational power of a HP in power level i
$P_{h,i,j}^{fix}$	Operational power of a HP in operational mode i,j
$\overline{P}_n^{EV}$	Maximum (dis-)charging power of EV n
$\overline{P}_h^{HR}$	Maximum operational power of a HR
$P_{h,t}^{L}$	Base load
P^{M}	Sufficiently large power
$P_{h,t}^{PV}$	Power generated by PV system
$P_{d,\tau}^{TSL}$	Operational power of TSL d in operational phase τ
$\dot{Q}_{h,i,j}^{fix}$	Heat flow of a HP in operational mode i,j
$\overline{\dot{Q}}_{h,i}^{HP}$	Upper bound for HP heat flow at power level i
$\dot{Q}_{h,t}^{sol}$	Solar irradiation
$\dot{Q}_{h,t}^{ST}$	Heat flow from ST system
$\dot{Q}_{h,t}^{w}$	Warm water demand
SOC_n^{end}	Lower bound for SOC of EV n at the end of the planning period
$\overline{SOC}_n^{EV}$	Upper bound for SOC of EV n
$\underline{SOC}_n^{EV}$	Lower bound for SOC of EV n
$SOC_{n,t}^{EV,req}$	Energy requirement for driving demand of EV n
UA_h^{H}	Thermal transmittance coefficient between a household and its ambience
UA_h^{HS}	Thermal transmittance coefficient between a household and its HS
$\Gamma_{h,t}^{HP}$	Binary parameter to (de-)activate the possibility of HP operation
Δt	Time step width
Δt^{HP}	Time step width for P2H system operational decisions
η_b^{BS}	BS (dis-)charging efficiency
η_n^{EV}	EV (dis-)charging efficiency
η_h^{HR}	HR efficiency
η_d^{TSL}	TSL efficiency
ϑ_t^{amb}	Ambient temperature
$\overline{\vartheta}_h^{c}$	Upper bound for household temperature within comfort time window
$\underline{\vartheta}_h^{c}$	Lower bound for household temperature within comfort time window
$\overline{\vartheta}_{j,h}^{cool}$	Upper bound for HP cooling supply temperature in termperature difference interval j
$\overline{\vartheta}_{h,t}^{H}$	Upper bound for household temperature
$\underline{\vartheta}_{h,t}^{H}$	Lower bound for household temperature
$\vartheta_h^{HP,sup}$	Supply point maximum temperature of a HP
$\overline{\vartheta}_{h,j}^{HS}$	Upper bound for HS temperature in temperature difference interval j
$\vartheta_h^{HS,end}$	HS temperature threshold at the end of the planning period
ϑ^{M}	Sufficiently high temperature
Λ_t^{int}	Binary parameter to (de-)activate the possibility of internal trading
Λ_t^{LM}	Binary parameter to (de-)activate the possibility of LM trading
λ_t^{LM}	LM energy price
λ_t^{WS}	WS energy price
Π^{HP}	Ratio of P2H system time step width and standard time step width

Data availability

Data will be made available on request.

References

[1] S. Kerscher, P. Arboleya, The key role of aggregators in the energy transition under the latest European regulatory framework, Int. J. Electr. Power Energy Syst. 134 (2022) 107–361, ISSN: 0142-0615, https://doi.org/10.1016/j.ijepes.2021.107361 (Online), Available: https://www.sciencedirect.com/science/article/pii/S0142061521006001

[2] N.S. Mahmood, A.A. Ajmi, S. Sarip, et al., Modeling energy management sustainability: smart integrated framework for future trends, Energy Rep. 8 (2022) 8027–8045, ISSN: 2352-4847, https://doi.org/10.1016/j.egyr.2022.06.023 (Online), Available: https://www.sciencedirect.com/science/article/pii/S2352484722011647

[3] A.M. Carreiro, H.M. Jorge, C.H. Antunes, Energy management systems aggregators: a literature survey, Renew. Sustain. Energy Rev. 73 (2017) 1160–1172, ISSN: 1364-0321, https://doi.org/10.1016/j.rser.2017.01.179 (Online), Available: https://www.sciencedirect.com/science/article/pii/S1364032117301776

[4] M.F. Zia, M. Benbouzid, E. Elbouchikhi, S.M. Muyeen, K. Techato, J. Guerrero, Microgrid transactive energy: review, architectures, distributed ledger technologies, and market analysis, IEEE Access 8, Jan (2020) 19410–19432, https://doi.org/10.1109/ACCESS.2020.2968402

[5] J. Iria, A. Coelho, F. Soares, Network-secure bidding strategy for aggregators under uncertainty, Sustain. Energy Grids Netw. 30 (2022) 100–666, ISSN: 2352-4677, https://doi.org/10.1016/j.segan.2022.100666 (Online), Available: https://www.sciencedirect.com/science/article/pii/S2352467722000340

[6] S. Backe, S. Zwickl-Bernhard, D. Schwabeneder, H. Auer, M. Korpås, A. Tomasgard, Impact of energy communities on the European electricity and heating system decarbonization pathway: comparing local and global flexibility responses, Appl. Energy 323 (2022) 119–470, ISSN: 0306-2619, https://doi.org/10.1016/j.apenergy.2022.119470 (Online), Available: https://www.sciencedirect.com/science/article/pii/S0306261922007954

[7] J. Stekli, L. Bai, U. Cali, U. Halden, M.F. Dynge, Distributed energy resource participation in electricity markets: a review of approaches, modeling, and enabling information and communication technologies, Energy Strategy Rev. 43 (2022) 100–940, ISSN: 2211-467X, https://doi.org/10.1016/j.esr.2022.100940 (Online), Available: https://www.sciencedirect.com/science/article/pii/S2211467X22001341

[8] J. Hu, G. Yang, K. Kok, Y. Xue, H.W. Bindner, Transactive control: a framework for operating power systems characterized by high penetration of distributed energy resources, J. Mod. Power Syst. Clean Energy 5 (3) (2017) 451–464, https://doi.org/10.1007/s40565-016-0228-1.

[9] The GridWise Architecture Council, Gridwise Transactive Energy Framework Version 1.0, 2015.

[10] O. Abrishambaf, F. Lezama, P. Faria, Z. Vale, Towards transactive energy systems: an analysis on current trends, Energy Strategy Rev. 26 (2019) 100–418, ISSN: 2211-467X, https://doi.org/10.1016/j.esr.2019.100418 (Online), Available: https://www.sciencedirect.com/science/article/pii/S2211467X19301105

[11] T. Capper, A. Gorbatcheva, M.A. Mustafa, et al., Peer-to-peer, community self-consumption, and transactive energy: a systematic literature review of local energy market models, Renew. Sustain. Energy Rev. 162 (2022) 112–403, ISSN: 1364-0321, https://doi.org/10.1016/j.rser.2022.112403 (Online), Available: https://www.sciencedirect.com/science/article/pii/S1364032122003112

[12] A.F. Cortés Borray, J. Merino, E. Torres, A. Garcés, J. Mazón, Centralised coordination of evs charging and PV active power curtailment over multiple aggregators in low voltage networks, Sustain. Energy Grids Netw. 27 (2021) 100–470, ISSN: 2352-4677, https://doi.org/10.1016/j.segan.2021.100470 (Online), Available: https://www.sciencedirect.com/science/article/pii/S2352467721000412

[13] J. Hu, G. Yang, C. Ziras, K. Kok, Aggregator operation in the balancing market through network-constrained transactive energy, IEEE Trans. Power Syst. 34 (5) (2019) 4071–4080, https://doi.org/10.1109/TPWRS.2018.2874255

[14] F. Lezama, J. Soares, P. Hernandez-Leal, M. Kaisers, T. Pinto, Z. Vale, Local energy markets: paving the path toward fully transactive energy systems, IEEE Trans. Power Syst. Jul (2018) 1–8, https://doi.org/10.1109/TPWRS.2018.2833959

[15] G.M. Casolino, L. D. Greco, A. Losi, Flexibility procurement for local ancillary services and provider aggregation perimeter in radial distribution systems, IEEE Access 12 (2024) 157383–157396, https://doi.org/10.1109/ACCESS.2024.3484675

[16] R. Moura, M.C. Brito, Prosumer aggregation policies, country experience and business models, Energy Policy 132 (2019) 820–830, ISSN: 0301-4215, https://doi.org/10.1016/j.enpol.2019.06.053 (Online), Available: https://www.sciencedirect.com/science/article/pii/S0301421519304239

[17] J.E. Contreras-Ocaña, M.A. Ortega-Vazquez, B. Zhang, Participation of an energy storage aggregator in electricity markets, IEEE Trans. Smart Grid 10 (2) (2019) 1171–1183, https://doi.org/10.1109/TSG.2017.2736787

[18] European Commission (2023). https://energy-communities-repository.ec.europa.eu/energy-communities-repository-about (Last viewed 12.12.2023).

[19] European Commission (2023). https://rural-energy-community-hub.ec.europa.eu/index (Last viewed 12.12.2023).

[20] C. Diaz-Londono, C.A. Correa-Florez, J. Vuelvas, A. Mazza, F. Ruiz, G. Chicco, Coordination of specialised energy aggregators for balancing service provision, Sustain. Energy Grids Netw. 32 (2022) 100–817, ISSN: 2352-4677, https://doi.org/10.1016/j.segan.2022.100817 (Online), Available: https://www.sciencedirect.com/science/article/pii/S2352467722001114

[21] Q. Wang, C. Zhang, Y. Ding, G. Xydis, J. Wang, J. Østergaard, Review of real-time electricity markets for integrating distributed energy resources and demand response, Appl. Energy 138 (2015) 695–706, ISSN: 0306-2619, https://doi.org/10.1016/j.apenergy.2014.10.048 (Online), Available: https://www.sciencedirect.com/science/article/pii/S0306261914010988

[22] P. Siano, G. De Marco, A. Rolán, V. Loia, A survey and evaluation of the potentials of distributed ledger technology for peer-to-peer transactive energy exchanges in local energy markets, IEEE Syst. J. 13 (3) (2019) 3454–3466, https://doi.org/10.1109/JSYST.2019.2903172.

[23] J. Li, Z. Wu, S. Zhou, H. Fu, X.-P. Zhang, Aggregator service for PV and battery energy storage systems of residential building, CSEE J. Power Energy Syst. 1 (4) (2015) 3–11, https://doi.org/10.17775/CSEEJPES.2015.00042.

[24] F. Wang, X. Ge, P. Yang, et al., Day-ahead optimal bidding and scheduling strategies for der aggregator considering responsive uncertainty under real-time pricing, Energy 213 (2020) 118–765, ISSN: 0360-5442, https://doi.org/10.1016/j.energy.2020.118765 (Online), Available: https://www.sciencedirect.com/science/article/pii/S0360544220318727

[25] P. Harsh, D. Das, Optimal coordination strategy of demand response and electric vehicle aggregators for the energy management of reconfigured grid-connected microgrid, Renew. Sustain. Energy Rev. 160 (2022) 112–251, ISSN: 1364-0321, https://doi.org/10.1016/j.rser.2022.112251 (Online), Available: https://www.sciencedirect.com/science/article/pii/S1364032122001721

[26] Z. Foroozandeh, S. Ramos, J. Soares, Z. Vale, M. Dias, Single contract power optimization: a novel business model for smart buildings using intelligent energy management, Int. J. Electr. Power Energy Syst. 135 (2022) 107–534, ISSN: 0142-0615, https://doi.org/10.1016/j.ijepes.2021.107534 (Online), Available: https://www.sciencedirect.com/science/article/pii/S0142061521007717

[27] S. Sadeghi, H. Jahangir, B. Vatandoust, M.A. Golkar, A. Ahmadian, A. Elkamel, Optimal bidding strategy of a virtual power plant in day-ahead energy and frequency regulation markets: a deep learning-based approach, Int. J. Electr. Power Energy Syst. 127 (2021) 106–646, ISSN: 0142-0615, https://doi.org/10.1016/j.ijepes.2020.106646 (Online), Available: https://www.sciencedirect.com/science/article/pii/S0142061520341910

[28] U. ur Rehman, M. Riaz, M.Y. Wani, A robust optimization method for optimizing day-ahead operation of the electric vehicles aggregator, Int. J. Electr. Power Energy Syst. 132 (2021) 107–179, ISSN: 0142-0615, https://doi.org/10.1016/j.ijepes.2021.107179. [Online]. Available: https://www.sciencedirect.com/science/article/pii/S014206152100418X

[29] T. Liu, X. Tan, B. Sun, Y. Wu, D.H. Tsang, Energy management of cooperative microgrids: a distributed optimization approach, Int. J. Electr. Power Energy Syst. 96 (2018) 335–346, ISSN: 0142-0615.

[30] J. Iria, P. Scott, A. Attarha, Network-constrained bidding optimization strategy for aggregators of prosumers, Energy 207 (2020) 118–266, ISSN: 0360-5442, https://doi.org/10.1016/j.energy.2020.118266 (Online), Available: https://www.sciencedirect.com/science/article/pii/S0360544220313736

[31] J. Iria, F. Soares, M. Matos, Optimal bidding strategy for an aggregator of prosumers in energy and secondary reserve markets, Appl. Energy 238 (2019) 1361–1372, ISSN: 0306-2619 (Online), Available: https://doi.org/10.1016/j.apenergy.2019.01.191

[32] T. Jin, H. Li, S.P.K. Prabha, Supply chain design for transactive energy operations in the nexus of manufacturing, microgrid and climate, J. Oper. Res. Soc. 73 (11) (2022) 2395–2411, https://doi.org/10.1080/01605682.2022.2035273.

[33] Z. Yi, Y. Xu, C. Wu, Improving operational flexibility of combined heat and power system through numerous thermal controllable residents aggregation, Int. J. Electr. Power Energy Syst. 130, Mar (2021) 106–841, https://doi.org/10.1016/j.ijepes.2021.106841.

[34] M. Di Somma, G. Graditi, P. Siano, Optimal bidding strategy for a der aggregator in the day-ahead market in the presence of demand flexibility, IEEE Trans. Ind. Electron. 66 (2) (2019) 1509–1519, https://doi.org/10.1109/TIE.2018.2829677.

[35] S.E. Ahmadi, D. Sadeghi, M. Marzband, A. Abusorrah, K. Sedraoui, Decentralized bi-level stochastic optimization approach for multi-agent multi-energy networked micro-grids with multi-energy storage technologies, Energy 245 (2022) 123–223, ISSN: 0360-5442, https://doi.org/10.1016/j.energy.2022.123223 (Online), Available: https://www.sciencedirect.com/science/article/pii/S0360544222001268

[36] K.J. Kircher, K.M. Zhang, Heat purchase agreements could lower barriers to heat pump adoption, Appl. Energy 286 (2021) 116–489, ISSN: 0306-2619, https://doi.org/10.1016/j.apenergy.2021.116489 (Online), Available: https://www.sciencedirect.com/science/article/pii/S0306261921000490

[37] A. Coelho, J. Iria, F. Soares, Network-secure bidding optimization of aggregators of multi-energy systems in electricity, gas, and carbon markets, Appl. Energy 301 (2021) 117–460, ISSN: 0306-2619, https://doi.org/10.1016/j.apenergy.2021.117460 (Online), Available: https://www.sciencedirect.com/science/article/pii/S0306261921008497

[38] Y. Vardanyan, A. Wolf, P. Bacher, et al., Optimal coordinated bidding of a profit-maximizing heat pump aggregator: the Dutch case, in: 2020 International Conference on Smart Grids and Energy Systems (SGES), 2020, pp. 71–76, https://doi.org/10.1109/SGES51519.2020.00020.

[39] K. Hoth, T. Steffen, B. Wiegel, et al., Holistic simulation approach for optimal operation of smart integrated energy systems under consideration of resilience, economics and sustainability, Infrastructures 6 (11) (2021).

[40] C.A. Correa-Florez, A. Michiorri, G. Kariniotakis, Optimal participation of residential aggregators in energy and local flexibility markets, IEEE Trans. Smart Grid 11 (2) (2020) 1644–1656, https://doi.org/10.1109/TSG.2019.2941687.

[41] P. Olivella-Rosell, E. Bullich-Massagué, M. Aragüés-Peñalba, et al., Optimization problem for meeting distribution system operator requests in local flexibility markets with distributed energy resources, Appl. Energy 210 (2018) 881–895, ISSN: 0306-2619, https://doi.org/10.1016/j.apenergy.2017.08.136 (Online), Available: https://www.sciencedirect.com/science/article/pii/S0306261917311522

[42] C. Calvillo, A. Sánchez-Miralles, J. Villar, F. Martín, Optimal planning and operation of aggregated distributed energy resources with market participation, Appl. Energy 182 (2016) 340–357, ISSN: 0306-2619, https://doi.org/10.1016/j.apenergy.2016.08.117 (Online), Available: https://www.sciencedirect.com/science/article/pii/S030626191631217X

[43] A. Paudel, L.P.M.I. Sampath, J. Yang, H.B. Gooi, Peer-to-peer energy trading in smart grid considering power losses and network fees, IEEE Trans. Smart Grid 11 (6) (2020) 4727–4737.
[44] SimBench (2023). https://simbench.de/de/datensaetze/ (Last viewed 12.12.2023).
[45] Deutsches Institut für Normung, Din En 12831-1 - Energy Performance of Buildings - Method for Calculation of the Design Heat Load, 2017.
[46] M. Lödl, G. Kerber, R. Witzmann, C. Hoffmann, M. Metzger, Abschätzung des photovoltaik-potentials auf dachflächen in deutschland, 2010. [Online]. Available: https://api.semanticscholar.org/CorpusID:168919237
[47] EV Database (2023) https://ev-database.org/car/1207/tesla-model-s-performance (Last viewed 12.07.2023).
[48] EV Database (2023) https://ev-database.org/car/1702/volkswagen-id4-pro-4motion (Last viewed 12.07.2023).
[49] EV Database (2023) https://ev-database.org/car/1650/volkswagen-e-up (Last viewed 12.07.2023).
[50] EV Database (2023) https://ev-database.org/car/1236/renault-zoe-ze40-r110 (Last viewed 12.07.2023).
[51] zenodo.org (2023) https://zenodo.org/records/5642902 (Last viewed 13.10.2023).
[52] D. Reinert, F. Prill, H. Frank, et al., DWD database reference for the global and regional ICON and ICON-EPS forecasting system, version 2.1.7, Deutscher Wetterdienst, Tech. Rep. (2021).
[53] SMARD Strommarktdaten (2023) https://www.smard.de/home/downloadcenter/download-marktdaten/ (Last viewed 13.10.2023).
[54] P. Dossow, T. Kern, S. von Roon, Entwicklungsrahmen der Haushaltsstrompreise in Deutschland, Tech. Rep., Forschungsgesellschaft für Energewirtschaft mbH, 2021.

Author biography

Kai Hoth received the B.Sc. degree in 2015 and the M.Sc. degree in 2017 from Leibniz University Hannover in the field of Engineering and Business Administration. He is currently pursuing the Ph.D. degree at Hamburg University of Technology in the field of Operations Research. He has previously worked as Managing Director of Spenjoy GmbH, as Engineering Consultant for ALTEN Technology GmbH and as Research Assistant at the Institute for Operations Management at the University of Hamburg. His current research interests include the aggregator-based optimization of renewable energy systems with a focus on local energy markets

Béla Wiegel received the B.Sc. degree in 2018 in the field of energy and environmental engineering and the M.Sc. degree in 2020 in the field of renewable energies with specialization in wind energy at the Hamburg University of Technology. He formerly has worked as student assistant in a research project in the field of energy technology. Currently he is pursuing the Ph.D. degree at Hamburg University of Technology. His current research interests are ancillary services and flexibility utilization in context of dynamics of future integrated distribution networks

Tizian Schug received the B.Sc. degree in 2019 from Friedrich-Alexander-University Erlangen-Nürnberg and the M.Sc. degree in 2022 from Hamburg University of Technology, both in the field of Engineering and Management. He is currently pursuing the Ph.D. degree at Hamburg University of Technology in the field of Operations Research. His current research interests include energy markets, flexibility in energy systems and machine learning for optimization problems

Kathrin Fischer received a Diploma in Mathematics, a Ph.D. degree in Management Science and a Habilitation in Business and Management from the University of Hamburg, Germany. Afterwards, she held a lectureship in Management Science at Aston Business School, Birmingham, UK, and professorships for Logistics in Hamburg and Vienna. Since 2009, she has been a Professor of Operations Research and Information Systems and Head of the Institute for Operations Research and Information Systems at the Hamburg University of Technology. Her major research interests are in the fields of humanitarian logistics, revenue management, location planning and energy systems. She has published articles in many OR-oriented journals, such as OR Spectrum, Transportation Science, Annals of OR and others